

Hybrid solar cells with ZnO-nanorods and dry processed small molecule absorber

W. Riedel, S. Wiesner, D. Greiner, V. Hinrichs, M. Rusu, and M. Ch. Lux-Steiner

Citation: [Applied Physics Letters](#) **104**, 173503 (2014); doi: 10.1063/1.4875255

View online: <http://dx.doi.org/10.1063/1.4875255>

View Table of Contents: <http://scitation.aip.org/content/aip/journal/apl/104/17?ver=pdfcov>

Published by the [AIP Publishing](#)

Articles you may be interested in

[Power losses in bilayer inverted small molecule organic solar cells](#)

Appl. Phys. Lett. **101**, 233903 (2012); 10.1063/1.4769440

[Influence of the polymer concentration on the electroluminescence of ZnO nanorod/polymer hybrid light emitting diodes](#)

J. Appl. Phys. **112**, 064324 (2012); 10.1063/1.4754542

[The photovoltaic performance of ZnO nanorods in bulk heterojunction solar cells](#)

J. Renewable Sustainable Energy **3**, 033105 (2011); 10.1063/1.3599838

[Thickness dependence of the MoO₃ blocking layers on ZnO nanorod-inverted organic photovoltaic devices](#)

Appl. Phys. Lett. **98**, 103305 (2011); 10.1063/1.3554381

[Organic/inorganic hybrid solar cells with vertically oriented ZnO nanowires](#)

Appl. Phys. Lett. **94**, 173107 (2009); 10.1063/1.3126955

High-Voltage Amplifiers

- Voltage Range from $\pm 50\text{V}$ to $\pm 60\text{kV}$
- Current to 25A

Electrostatic Voltmeters

- Contacting & Non-contacting
- Sensitive to 1mV
- Measure to 20kV



ENABLING RESEARCH AND
INNOVATION IN DIELECTRICS,
ELECTROSTATICS,
MATERIALS, PLASMAS AND PIEZOS



www.trekinc.com

TREK, INC. 190 Walnut Street, Lockport, NY 14094 USA • Toll Free in USA 1-800-FOR-TREK • (t):716-438-7555 • (f):716-201-1804 • sales@trekinc.com



Hybrid solar cells with ZnO-nanorods and dry processed small molecule absorber

W. Riedel, S. Wiesner, D. Greiner, V. Hinrichs, M. Rusu,^{a)} and M. Ch. Lux-Steiner
*Institut für Heterogene Materialsysteme, Helmholtz-Zentrum Berlin für Materialien und Energie,
 Lise-Meitner Campus, Hahn-Meitner-Platz 1, 14109 Berlin, Germany*

(Received 10 February 2014; accepted 25 April 2014; published online 2 May 2014)

We demonstrate hybrid solar cells with ZnO-nanorods (ZnO-NRs) prepared by a low temperature electrochemical method and small molecule organic absorber processed by dry organic vapor phase deposition. A homogeneous coverage of ZnO-NRs by the blend absorber consisting of zinc phthalocyanine (ZnPc) as donor and of fullerene C₆₀ as acceptor is best realized when a thin C₆₀ layer is first inserted at the ZnO-NR/ZnPc:C₆₀ interface. ZnO-NR/C₆₀/ZnPc:C₆₀/MoO₃/Ag solar cell devices with efficiencies of 2.8% under an illumination of 100 mW/cm² at 25 °C are demonstrated.
 © 2014 AIP Publishing LLC. [<http://dx.doi.org/10.1063/1.4875255>]

In the past decade, organic photovoltaic (OPV) devices have been extensively developed due to their potential low cost, light weight, easy to up-scale, and compatibility with flexible substrates. The efficiency of small molecule based OPV cells has been continuously improved and reached 5% on single solar cells¹ and 12.0% on tandem devices.² This remarkable progress has been attained through the use of new organic materials, better band alignment at organic and hybrid interfaces as well as through the development of new absorber structures including donor-acceptor (D:A) blend layers. The latter approach has been introduced in order (i) to match the size of the donor and/or acceptor domains to the exciton diffusion length (which is typically of less than 40 nm)³ and (ii) to be able to increase the absorber thickness to the optical absorption length (which is of the order of few hundreds of nanometers). However, while the first condition is easily achieved, the realization of the second one is challenging. The point is that dead end pathways impede the carrier flow and thus increase the series resistance of devices. This results in reduced fill factors (FFs) which in the end detrimentally affect the solar cell efficiency.

In order to overcome the latter problem, it has been recently proposed to prepare OPV cells with blend organic absorbers deposited on nanostructured oxide semiconductors such as ZnO with vertically aligned nanorods (nanofibers).⁴ By using this approach, the active area of the absorber increases. In addition, effective charge carrier transport pathways are created. In particular, electrons are effectively transported via ZnO-nanorods (ZnO-NRs), since their mobility of approx. 100 cm² × V⁻¹ × s⁻¹ is by several orders of magnitude higher than that found in organic semiconductors. By using this approach, OPV cells based on composite blends of poly(3-hexylthiophene) (P3HT) and (6,6)-phenyl C₆₁ butyric acid methyl ester (PCBM) with efficiencies of 2.03% (Ref. 4) were prepared by means of a wet spin-coating method. Similar concept was applied for the preparation of polymer-based OPV devices with efficiencies of 3.9%.⁵

In this work, we demonstrate hybrid solar cells with an efficiency of 2.8% (under 100 mW/cm² at 25 °C) which comprise ZnO-NRs and dry-processed small molecule organic absorber consisting of a blend of zinc phthalocyanine (ZnPc) as donor and of the fullerene C₆₀ as acceptor. When compared to conventional OPV cells, the polarity of electrodes in the investigated device is inverted, the front ZnO transparent electrode acting as cathode. The ohmic contact at the cathode/C₆₀ interface is realized by a matching ZnO-NR work function. The effective charge selectivity at the interface between ZnPc:C₆₀ blend layer and Ag back contact is ensured by the insertion of a transition metal oxide (TMO) layer such as MoO₃ at this interface. MoO₃ was previously proven to successfully replace poly(3,4-ethylene dioxythiophene):(polystyrene sulfonic acid) PEDOT:PSS as the hole selective buffer layer in polymer photovoltaic cells.⁶ Our experiments demonstrated an effective replacement for the wet-processed p-type PEDOT:PSS layer by an evaporated MoO₃ thin film for small molecule based conventional planar solar cells: even higher solar cell PV parameters were recorded on solar cells with MoO₃ (see Table I).

The morphology of thin films and cross-section views of solar cells were investigated by scanning electron microscopy (SEM) using a Gemini LEO 1530 microscope at an operating voltage of typically 5.0 kV. Optical transmission and reflection measurements were carried out at room temperature in air by a Varian Cary 500 UV-Vis-NIR spectrophotometer. The work function of ZnO-NRs was determined from high binding energy cut-off (HBEC) spectra of x-ray photoelectron spectroscopy (XPS) measurements. The XPS measurements were carried out under UHV conditions (base pressure ~10⁻¹⁰ millibars). The data were recorded using Mg K_α x-ray radiation (1253.6 eV, source Specs XR 50) and a Specs Phoibos 100 electron spectrometer. The electrical parameters—the series resistance, R_s, and the parallel resistance, R_p, of the OPV devices were determined by fitting the dark current-voltage (J-V) curves to the one diode model described by the extended Shockley equation⁷ which is applicable for phthalocyanine/fullerene based solar cell devices.⁸ The PV parameters—power conversion efficiency

^{a)}Author to whom correspondence should be addressed. Electronic mail: rusu@helmholtz-berlin.de

TABLE I. PV parameters of conventional glass/ITO/hole transport layer (HTL)/80 nm ZnPc:C₆₀/100 nm Mg:Ag solar cells (device area 0.063 cm²).

HTL	Eff (%)	V _{oc} (mV)	J _{sc} (mA/cm ²)	FF (%)
MoO ₃	4.5	530	17.1	49.7
PEDOT:PSS	3.7	520	15.9	44.6

(Eff), short-circuit current density (J_{sc}), open circuit voltage (V_{oc}), and FF were determined from J-V measurements performed under an illumination of 100 mW/cm² (Ha-lamp) at 25 °C.

ZnO-NRs were grown by electrodeposition on indium tin oxide (ITO) substrates from an aqueous solution of 5 mM Zn(NO₃)₂ and 5 mM NH₄NO₃ at a temperature of 75 °C. Before ZnO deposition, ITO substrates were covered by a seed layer (SL) of 30 nm sputtered intrinsic ZnO (i-ZnO). The ZnO-NR diameter and length were adjusted by varying the deposition time. Further details of the ZnO-NR preparation are published elsewhere.^{9,10}

Figure 1 shows the morphology of ZnO-NRs. The as-grown ZnO-NRs represent high quality crystallites and exhibit a hexagonal structure, as demonstrated by x-ray diffraction analysis (not shown). The deposition results are highly reproducible: the average diameter and length of as-grown ZnO-NRs can be well adjusted between 50 and 100 nm and between 180 and 600 nm, respectively, by varying the deposition time between 400 and 1500 s. Due to a slight tilt of the ZnO-NRs, the spacing between ZnO-NRs varies from few nanometers to few hundreds of nanometers.

Figure 2(a) shows the transmittance and reflectance spectra of ZnO-NRs/i-ZnO seed layer/ITO/glass structures and that of reference ITO/glass and planar ZnO doped by Aluminium (ZnO:Al)/glass stacks measured against air with the light incident on the glass side. The transmission of ZnO-NRs in the wavelength range of 400–800 nm is on average higher than 83% and thus surpassing that of the

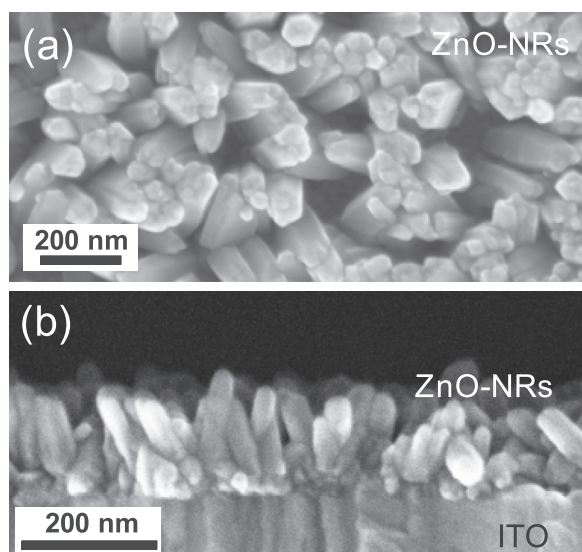


FIG. 1. SEM images of ZnO-NRs deposited during 700 s on ITO/glass substrates covered by a 30 nm sputtered i-ZnO nucleation layer: (a) Top view. (b) Cross-section.

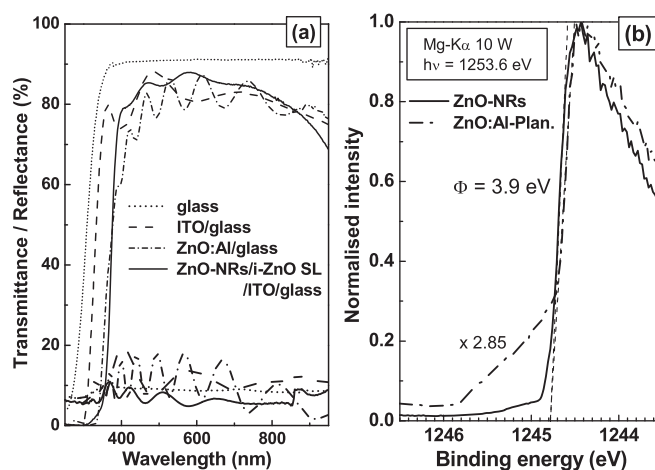


FIG. 2. (a) Transmittance and reflectance of a ZnO-NRs/i-ZnO nucleation layer/ITO/glass structure in comparison to that of glass, ITO/glass, and ZnO:Al/glass stacks. (b) HBEC spectra of ZnO-NRs and planar ZnO:Al. The work function, Φ , is determined by linearly fitting the spectra and extrapolating to zero. To account for the analyzer broadening of 0.2 eV, the obtained HBEC values at the intersection points were corrected by 0.1 eV.

planar ITO and ZnO:Al thin films (ITO (5 Ω/□): 82% and ZnO:Al (5 Ω/□): 81%). In addition, ZnO-NRs show in the same wavelength range the lowest average reflection of about 7%.

From XPS spectra in Fig. 2(b), work function values of 3.9 ± 0.1 eV were determined for the as-prepared ZnO-NRs, which are similar to that of planar ZnO:Al prepared by sputtering for inorganic solar cells.¹¹ This value matches perfectly the work function value found for ohmic Mg-Ag contacts to C₆₀ and that of selective Mg-Ag cathodes of solar cells based on CuPc:C₆₀ or ZnPc:C₆₀ absorber layers.^{12,13} Thus, the as-prepared ZnO-NRs can be directly applied (without any additional surface treatments or use of buffer layers) as cathodes in (Cu or Zn)Pc:C₆₀ based solar cells.

Organic materials were deposited by dry organic vapor phase deposition (OVPD)^{13,14} which is a diffusion controlled process and thus suitable for deposition of thin films on highly structured surfaces. Nevertheless, cape-like growth of ZnPc:C₆₀ layers on ZnO-NRs as, for example, in Fig. 3(a) was observed for deposition pressures between 0.5 and 1.0 millibars and substrate temperatures between 163 °C and 126 °C, respectively. Cluster formation was observed at low pressures and high temperatures, e.g., at 0.3 millibars and 195 °C (Fig. 3(b)). Coverage homogeneity was improved when an additional 50 nm C₆₀ layer was first deposited on top of ZnO-NRs at a deposition pressure of 0.6 millibars and a substrate temperature of 151 °C. The cross-section SEM image in Fig. 3(c) confirms the improved conformal coverage of highly structured ZnO-NRs. The device schematic in Fig. 3(d) shows the materials involved and explains the charge carrier generation under illumination and transport to electrodes: generated excitons are separated at D:A interfaces and thus free charge carriers are produced; electrons are then consecutively transported via C₆₀ acceptor domains, C₆₀ layer and ZnO-NRs to the front contact. At the same time, holes reach the back contact by travelling via ZnPc donor domains.

Optical measurements of the complete devices show a decreased reflectance and thus, an increased absorbance

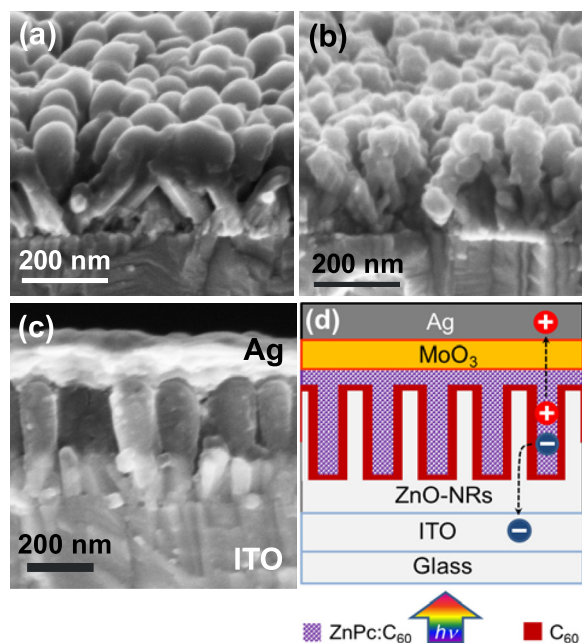


FIG. 3. (a) and (b) SEM images of CuPc:C₆₀ blend layer deposited by OVPD on ZnO-NRs/i-ZnO nucleation layer/ITO/glass structures at deposition pressures and substrate temperatures of (a) 0.5 millibars and 165 °C and (b) 0.3 millibars and 195 °C. (c) SEM micrograph of a complete solar cell device with a structure as presented in Fig. 3(d). A 50 nm C₆₀ thin film and a 80 nm blend ZnPc:C₆₀ layer were deposited by OVPD at a deposition pressure of 0.6 millibars and a substrate temperature of 151 °C.

($A = 1 - R$) for the solar cell with ZnO-NRs compared to the device with the planar ZnO:Al (Fig. 4(a)). Between 350 nm and 950 nm, clearly interference fringes are reduced and the average absorbance of the optical stack increases by about 21% indicating improved absorption due to the anti-reflective effect of the ZnO-NRs and thus suggesting a higher exciton generation in the device with ZnO-NRs.

The dark and illuminated J-V curves of the solar cell device with ZnO-NRs shown in Fig. 3(c) are presented in Fig. 4(b) in comparison to a simultaneously prepared device on planar ZnO:Al. The electric and PV parameters derived from the respective J-V curves are summarized in Table II. An efficiency of 2.8% is demonstrated for the

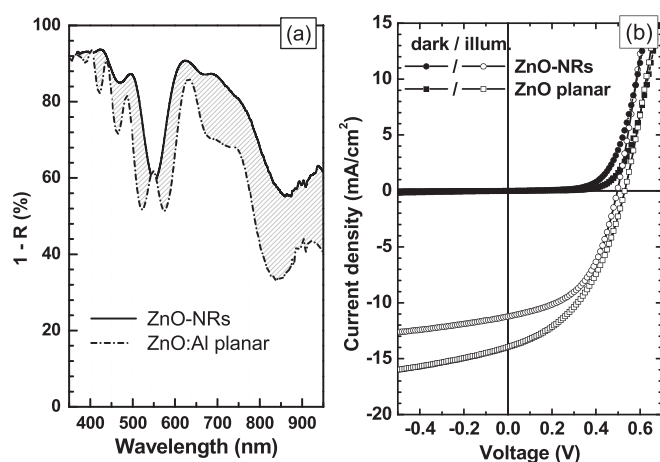


FIG. 4. (a) Absorbance ($A = 1 - R$) of ZnO-NRs vs. ZnO:Al-planar/50 nm C₆₀/80 nm ZnPc:C₆₀/10 nm MoO₃/100 nm Ag solar cells (device area 0.30 cm²). (b) Dark and illuminated J-V curves of devices in Fig. 4(a).

TABLE II. PV and electric parameters of inverted ZnO-NRs vs. ZnO:Al-planar/50 nm C₆₀/80 nm ZnPc:C₆₀/10 nm MoO₃/100 nm Ag solar cells (device area 0.30 cm²).

TCO ^a	Eff (%)	V _{oc} (mV)	J _{sc} (mA/cm ²)	FF (%)	R _s (Ω × cm ²)	R _p (kΩ × cm ²)
ZnO-NRs	2.8	500	11.2	50.0	4.73	4.4
ZnO:Al planar	3.2	530	14.0	43.1	5.33	10.2

^aTransparent conductive oxide.

ZnO-NR solar cell. Despite a higher fill factor and a reduced series resistance, this efficiency is still lower than that of the planar PV device. The reason is that the recorded J_{sc} is much lower compared to that of the planar device, in contrast to the result expected from the absorbance characteristics.

The contradiction between optical and photoelectric data is partially explained by the fact that the additional absorption does not necessarily result in charge carrier collection: First, the lack of an improved J_{sc} for the device with ZnO-NRs despite the increased total absorbance may partially be due to light absorption in layers which do not result in charge carrier generation, e.g., in ZnO SL. Second, charge carriers may be lost due to recombination, as suggested by the reduced parallel resistance (see Table II). Recombination in the solar cell with ZnO-NRs may be increased compared to the device with planar ZnO:Al due to additional interfaces, e.g., ITO/i-ZnO SL and i-ZnO SL/ZnO-NRs. Moreover, further recombination losses may occur due to the absence of an interdigitated contact structure: as seen from Figs. 3(c) and 3(d), the back contact does not completely follow the morphology of the organic film on ZnO-NRs. Therefore, an increased recombination is expected due to in parts enlarged drift paths of holes to the back contact. Preparation of devices with an optimized morphology of the back contact will be a subject of further investigations.

In conclusion, hybrid ZnO-NR/C₆₀/ZnPc:C₆₀/MoO₃/Ag solar cells with efficiencies of 2.8% have been demonstrated. A homogeneous coverage of ZnO-NRs by organic layers was achieved by the application of the dry OVPD process. A C₆₀ thin film between ZnO-NRs and the ZnPc:C₆₀ blend layer improves the coverage uniformity along the nanorods.

The authors gratefully acknowledge the support of the Helmholtz-Gemeinschaft Deutscher Forschungszentren e.V. (HGF) (project “Hybrid-PV”).

¹J. Xue, B. P. Rand, S. Uchida, and S. R. Forrest, *Adv. Mater.* **17**(1), 66 (2005).

²T. Ameri, N. Li, and Ch. J. Brabec, *Energy Environ. Sci.* **6**, 2390 (2013).

³P. Peumans, A. Yakimov, and S. R. Forrest, *J. Appl. Phys.* **93**, 3693 (2003).

⁴D. C. Olson, J. Piris, R. T. Collins, S. E. Shaheen, and D. S. Ginley, *Thin Solid Films* **496**, 26 (2006).

⁵K. Takanezawa, K. Tajima, and K. Hashimoto, *Appl. Phys. Lett.* **93**, 063308 (2008).

⁶V. Shrotriya, G. Li, Y. Yao, C.-W. Chu, and Y. Yang, *Appl. Phys. Lett.* **88**, 073508 (2006).

⁷R. H. Bube and A. L. Fahrenbruch, *Advances in Electronics and Electron Physics* (Academic Press, New York, 1981), p. 163.

- ⁸B. P. Rand, D. P. Burk, and S. R. Forrest, *Phys. Rev. B* **75**, 115327 (2007).
- ⁹Y. Tang, J. Chen, D. Greiner, L. A  , R. Baier, J. Lehmann, S. Sadewasser, and M. Ch. Lux-Steiner, *J. Phys. Chem. C* **115**, 5239 (2011).
- ¹⁰W. Ludwig, W. Ohm, J.-M. Correa-Hoyos, Y. Zhao, M. Ch. Lux-Steiner, and S. Gledhill, *Phys. Status Solidi A* **210**, 1557 (2013).
- ¹¹M. Rusu, F. Kraffert, S. Wiesner, W. Schindler, K. Fostiropoulos, and M. Ch. Lux-Steiner, *Energy Procedia* **31**, 96 (2012).
- ¹²M. Rusu, S. Wiesner, I. Lauer mann, Ch. -H. Fischer, K. Fostiropoulos, J. N. Audinot, Y. Fleming, and M. Ch. Lux-Steiner, *Appl. Phys. Lett.* **97**, 073504 (2010).
- ¹³M. Rusu, S. Wiesner, T. Mete, H. Blei, N. Meyer, M. Heuken, M. Ch. Lux-Steiner, and K. Fostiropoulos, *Renewable Energy* **33**, 254 (2008).
- ¹⁴M. Rusu, J. Gasiorowski, S. Wiesner, N. Meyer, M. Heuken, K. Fostiropoulos, and M. Ch. Lux-Steiner, *Thin Solid Films* **516**, 7160 (2008).